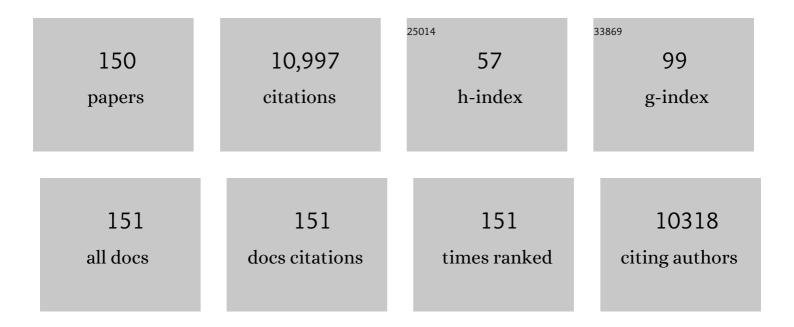
Jianrong Chen

List of Publications by Year in descending order

Source: https://exaly.com/author-pdf/11889902/publications.pdf Version: 2024-02-01



#	Article	IF	CITATIONS
1	A critical review of extracellular polymeric substances (EPSs) in membrane bioreactors: Characteristics, roles in membrane fouling and control strategies. Journal of Membrane Science, 2014, 460, 110-125.	4.1	583
2	A review on anaerobic membrane bioreactors: Applications, membrane fouling and future perspectives. Desalination, 2013, 314, 169-188.	4.0	545
3	Highly Luminescent Nâ€Doped Carbon Quantum Dots as an Effective Multifunctional Fluorescence Sensing Platform. Chemistry - A European Journal, 2014, 20, 2254-2263.	1.7	407
4	Si-Doped Carbon Quantum Dots: A Facile and General Preparation Strategy, Bioimaging Application, and Multifunctional Sensor. ACS Applied Materials & Interfaces, 2014, 6, 6797-6805.	4.0	323
5	Determination of cadmium, copper, lead and zinc in water samples by flame atomic absorption spectrometry after cloud point extraction. Analytica Chimica Acta, 2001, 450, 215-222.	2.6	319
6	Membrane Bioreactors for Industrial Wastewater Treatment: A Critical Review. Critical Reviews in Environmental Science and Technology, 2012, 42, 677-740.	6.6	256
7	B-doped carbon quantum dots as a sensitive fluorescence probe for hydrogen peroxide and glucose detection. Analyst, The, 2014, 139, 2322-2325.	1.7	252
8	Determination of cadmium(II), cobalt(II), nickel(II), lead(II), zinc(II), and copper(II) in water samples using dual-cloud point extraction and inductively coupled plasma emission spectrometry. Journal of Hazardous Materials, 2012, 239-240, 206-212.	6.5	231
9	Membrane fouling in a membrane bioreactor: High filtration resistance of gel layer and its underlying mechanism. Water Research, 2016, 102, 82-89.	5.3	209
10	A unified thermodynamic mechanism underlying fouling behaviors of soluble microbial products (SMPs) in a membrane bioreactor. Water Research, 2019, 149, 477-487.	5.3	203
11	Carbon Quantum Dots-Based Recyclable Real-Time Fluorescence Assay for Alkaline Phosphatase with Adenosine Triphosphate as Substrate. Analytical Chemistry, 2015, 87, 2966-2973.	3.2	201
12	Facile synthesis of P-doped carbon quantum dots with highly efficient photoluminescence. RSC Advances, 2014, 4, 5465.	1.7	190
13	Surface functionalization of graphene quantum dots with small organic molecules from photoluminescence modulation to bioimaging applications: an experimental and theoretical investigation. RSC Advances, 2013, 3, 14571.	1.7	189
14	Determination of cobalt and nickel in water samples by flame atomic absorption spectrometry after cloud point extraction. Analytica Chimica Acta, 2001, 434, 325-330.	2.6	181
15	New insights into membrane fouling in a submerged anaerobic membrane bioreactor based on characterization of cake sludge and bulk sludge. Bioresource Technology, 2011, 102, 2373-2379.	4.8	176
16	Determination of lead in water samples by graphite furnace atomic absorption spectrometry after cloud point extraction. Talanta, 2005, 67, 992-996.	2.9	169
17	Mechanistic insights into alginate fouling caused by calcium ions based on terahertz time-domain spectra analyses and DFT calculations. Water Research, 2018, 129, 337-346.	5.3	168
18	Feasibility evaluation of submerged anaerobic membrane bioreactor for municipal secondary wastewater treatment. Desalination, 2011, 280, 120-126.	4.0	160

#	Article	IF	CITATIONS
19	A high-performance hybrid supercapacitor with NiO derived NiO@Ni-MOF composite electrodes. Electrochimica Acta, 2020, 340, 135956.	2.6	157
20	Inkjet printing of dopamine followed by UV light irradiation to modify mussel-inspired PVDF membrane for efficient oil-water separation. Journal of Membrane Science, 2021, 619, 118790.	4.1	149
21	Molecular Engineering toward Pyrrolic Nâ€Rich Mâ€N ₄ (M = Cr, Mn, Fe, Co, Cu) Singleâ€Atom Sites for Enhanced Heterogeneous Fentonâ€Like Reaction. Advanced Functional Materials, 2021, 31, 2007877.	7.8	139
22	Fouling mechanisms of gel layer in a submerged membrane bioreactor. Bioresource Technology, 2014, 166, 295-302.	4.8	133
23	Effects of hydrophilicity/hydrophobicity of membrane on membrane fouling in a submerged membrane bioreactor. Bioresource Technology, 2015, 175, 59-67.	4.8	130
24	Luminescent Nanoswitch Based on Organic-Phase Copper Nanoclusters for Sensitive Detection of Trace Amount of Water in Organic Solvents. Analytical Chemistry, 2016, 88, 7429-7434.	3.2	122
25	A new insight into membrane fouling mechanism in submerged membrane bioreactor: Osmotic pressure during cake layer filtration. Water Research, 2013, 47, 2777-2786.	5.3	117
26	A fluorometric assay for alkaline phosphatase activity based on β-cyclodextrin-modified carbon quantum dots through host-guest recognition. Biosensors and Bioelectronics, 2016, 83, 274-280.	5.3	117
27	Efficient degradation and mineralization of antibiotics via heterogeneous activation of peroxymonosulfate by using graphene supported single-atom Cu catalyst. Chemical Engineering Journal, 2020, 394, 124904.	6.6	117
28	Different fouling propensities of loosely and tightly bound extracellular polymeric substances (EPSs) and the related fouling mechanisms in a membrane bioreactor. Chemosphere, 2020, 255, 126953.	4.2	112
29	A conductive PVDF-Ni membrane with superior rejection, permeance and antifouling ability via electric assisted in-situ aeration for dye separation. Journal of Membrane Science, 2019, 581, 401-412.	4.1	107
30	Graphene "bridge―in transferring hot electrons from plasmonic Ag nanocubes to TiO2 nanosheets for enhanced visible light photocatalytic hydrogen evolution. Applied Catalysis B: Environmental, 2018, 220, 182-190.	10.8	105
31	Reversible Fluorescent Nanoswitch Based on Carbon Quantum Dots Nanoassembly for Real-Time Acid Phosphatase Activity Monitoring. Analytical Chemistry, 2015, 87, 7332-7339.	3.2	103
32	Effects of molecular weight distribution of soluble microbial products (SMPs) on membrane fouling in a membrane bioreactor (MBR): Novel mechanistic insights. Chemosphere, 2020, 248, 126013.	4.2	97
33	Enhanced visible-light-driven photocatalysis from WS ₂ quantum dots coupled to BiOCl nanosheets: synergistic effect and mechanism insight. Catalysis Science and Technology, 2018, 8, 201-209.	2.1	95
34	Highly efficient removal of chlorotetracycline from aqueous solution using graphene oxide/TiO 2 composite: Properties and mechanism. Applied Surface Science, 2017, 425, 765-775.	3.1	94
35	New insights into bisphenols removal by nitrogen-rich nanocarbons: Synergistic effect between adsorption and oxidative degradation. Journal of Hazardous Materials, 2018, 345, 123-130.	6.5	93
36	Ultrahigh sorption and reduction of Cr(VI) by two novel core-shell composites combined with Fe3O4 and MoS2. Journal of Hazardous Materials, 2019, 379, 120797.	6.5	87

#	Article	IF	CITATIONS
37	Quantification of interfacial energies associated with membrane fouling in a membrane bioreactor by using BP and GRNN artificial neural networks. Journal of Colloid and Interface Science, 2020, 565, 1-10.	5.0	86
38	Thermodynamic analysis of membrane fouling in a submerged membrane bioreactor and its implications. Bioresource Technology, 2013, 146, 7-14.	4.8	83
39	Fabrication of CoFe2O4–graphene nanocomposite and its application in the magnetic solid phase extraction of sulfonamides from milk samples. Talanta, 2015, 144, 1279-1286.	2.9	83
40	Surface modification of polyvinylidene fluoride (PVDF) membrane via radiation grafting: novel mechanisms underlying the interesting enhanced membrane performance. Scientific Reports, 2017, 7, 2721.	1.6	80
41	Luminescent Aggregated Copper Nanoclusters Nanoswitch Controlled by Hydrophobic Interaction for Real-Time Monitoring of Acid Phosphatase Activity. Analytical Chemistry, 2016, 88, 11575-11583.	3.2	79
42	Realization of quantifying interfacial interactions between a randomly rough membrane surface and a foulant particle. Bioresource Technology, 2017, 226, 220-228.	4.8	77
43	Bridge engineering in photocatalysis and photoelectrocatalysis. Nanoscale, 2020, 12, 5764-5791.	2.8	77
44	Determination of manganese in water samples by flame atomic absorption spectrometry after cloud point extraction. Analyst, The, 2001, 126, 534-537.	1.7	75
45	A fluorometric assay for acetylcholinesterase activity and inhibitor screening with carbon quantum dots. Sensors and Actuators B: Chemical, 2016, 222, 879-886.	4.0	73
46	Impact of resuscitation promoting factor (Rpf) in membrane bioreactor treating high-saline phenolic wastewater: Performance robustness and Rpf-responsive bacterial populations. Chemical Engineering Journal, 2019, 357, 715-723.	6.6	73
47	Sustainable biodegradation of phenol by immobilized Bacillus sp. SAS19 with porous carbonaceous gels as carriers. Journal of Environmental Management, 2018, 222, 185-189.	3.8	68
48	A novel strategy to develop antifouling and antibacterial conductive Cu/polydopamine/polyvinylidene fluoride membranes for water treatment. Journal of Colloid and Interface Science, 2018, 531, 493-501.	5.0	68
49	Enhanced catalytic degradation of bisphenol A by hemin-MOFs supported on boron nitride via the photo-assisted heterogeneous activation of persulfate. Separation and Purification Technology, 2019, 229, 115822.	3.9	68
50	Cocatalyst Engineering in Piezocatalysis: A Promising Strategy for Boosting Hydrogen Evolution. ACS Applied Materials & Interfaces, 2021, 13, 15305-15314.	4.0	68
51	Determination of bisphenol A and naphthols in river water samples by capillary zone electrophoresis after cloud point extraction. Talanta, 2011, 85, 488-492.	2.9	67
52	A new method for modeling rough membrane surface and calculation of interfacial interactions. Bioresource Technology, 2016, 200, 451-457.	4.8	66
53	Twin defects engineered Pd cocatalyst on C ₃ N ₄ nanosheets for enhanced photocatalytic performance in CO ₂ reduction reaction. Nanotechnology, 2017, 28, 484003.	1.3	63
54	Insight into the mechanisms for hexavalent chromium reduction and sulfisoxazole degradation catalyzed by graphitic carbon nitride: The Yin and Yang in the photo-assisted processes. Chemosphere, 2019, 221, 166-174.	4.2	63

#	Article	IF	CITATIONS
55	Interface engineering on Janus Pd–Au heterojunction co-catalysts for selective photocatalytic reduction of CO ₂ to CH ₄ . Journal of Materials Chemistry A, 2019, 7, 5266-5276.	5.2	61
56	Mo-doped Co3O4 ultrathin nanosheet arrays anchored on nickel foam as a bi-functional electrode for supercapacitor and overall water splitting. Journal of Colloid and Interface Science, 2021, 602, 355-366.	5.0	61
57	Defects-type three-dimensional Co3O4 nanomaterials for energy conversion and low temperature energy storage. Applied Surface Science, 2021, 546, 149064.	3.1	60
58	Precise regulation of pyrroleâ€ŧype singleâ€atom Mnâ€N ₄ sites for superior pHâ€universal oxygen reduction. , 2021, 3, 856-865.		60
59	Physicochemical correlations between membrane surface hydrophilicity and adhesive fouling in membrane bioreactors. Journal of Colloid and Interface Science, 2017, 505, 900-909.	5.0	56
60	Bamboo-like carbon nanotubes derived from colloidal polymer nanoplates for efficient removal of bisphenol A. Journal of Materials Chemistry A, 2016, 4, 15450-15456.	5.2	55
61	Enhancement of polychlorinated biphenyl biodegradation by resuscitation promoting factor (Rpf) and Rpf-responsive bacterial community. Chemosphere, 2021, 263, 128283.	4.2	55
62	Order engineering on the lattice of intermetallic PdCu co-catalysts for boosting the photocatalytic conversion of CO ₂ into CH ₄ . Journal of Materials Chemistry A, 2018, 6, 17444-17456.	5.2	54
63	Bacterial community shifts evaluation in the sediments of Puyang River and its nitrogen removal capabilities exploration by resuscitation promoting factor. Ecotoxicology and Environmental Safety, 2019, 179, 188-197.	2.9	54
64	Cation-driven luminescent self-assembled dots of copper nanoclusters with aggregation-induced emission for β-galactosidase activity monitoring. Journal of Materials Chemistry B, 2017, 5, 5120-5127.	2.9	53
65	Factors influencing DBPs occurrence in tap water of Jinhua Region in Zhejiang Province, China. Ecotoxicology and Environmental Safety, 2019, 171, 813-822.	2.9	53
66	Nanosized N-doped graphene oxide with visible fluorescence in water for metal ion sensing. Journal of Materials Chemistry, 2011, 21, 17635.	6.7	52
67	Efficient elimination of Cr(VI) from aqueous solutions using sodium dodecyl sulfate intercalated molybdenum disulfide. Ecotoxicology and Environmental Safety, 2019, 175, 251-262.	2.9	52
68	Facile synthesis of halogenated carbon quantum dots as an important intermediate for surface modification. RSC Advances, 2013, 3, 9625.	1.7	50
69	Molybdenum doped induced amorphous phase in cobalt acid nickel for supercapacitor and oxygen evolution reaction. Journal of Colloid and Interface Science, 2022, 606, 1695-1706.	5.0	50
70	Graphene-Fe ₃ O ₄ as a magnetic solid-phase extraction sorbent coupled to capillary electrophoresis for the determination of sulfonamides in milk. Journal of Separation Science, 2016, 39, 3818-3826.	1.3	48
71	Simultaneous determination of dopamine and uric acid using layer-by-layer graphene and chitosan assembled multilayer films. Talanta, 2013, 117, 359-365.	2.9	47
72	Resuscitation of functional bacterial community for enhancing biodegradation of phenol under high salinity conditions based on Rpf. Bioresource Technology, 2018, 261, 394-402.	4.8	47

#	Article	IF	CITATIONS
73	Enhanced performance of a submerged membrane bioreactor with powdered activated carbon addition for municipal secondary effluent treatment. Journal of Hazardous Materials, 2011, 192, 1509-1514.	6.5	46
74	Organic dye doped graphitic carbon nitride with a tailored electronic structure for enhanced photocatalytic hydrogen production. Catalysis Science and Technology, 2019, 9, 502-508.	2.1	45
75	Viable but Nonculturable State of Yeast <i>Candida</i> sp. Strain LN1 Induced by High Phenol Concentrations. Applied and Environmental Microbiology, 2021, 87, e0111021.	1.4	45
76	Precursors for brominated haloacetic acids during chlorination and a new useful indicator for bromine substitution factor. Science of the Total Environment, 2020, 698, 134250.	3.9	44
77	Osmotic pressure effect on membrane fouling in a submerged anaerobic membrane bioreactor and its experimental verification. Bioresource Technology, 2012, 125, 97-101.	4.8	43
78	Effective partial denitrification of biological effluent of landfill leachate for Anammox process: Start-up, influencing factors and stable operation. Science of the Total Environment, 2022, 807, 150975.	3.9	42
79	Pollutant removal and membrane fouling in an anaerobic submerged membrane bioreactor for real sewage treatment. Water Science and Technology, 2014, 69, 1712-1719.	1.2	40
80	Simultaneous Detection of Multiple DNA Targets by Integrating Dual olor Graphene Quantum Dot Nanoprobes and Carbon Nanotubes. Chemistry - A European Journal, 2014, 20, 16065-16069.	1.7	40
81	Aerobic degradation of 3,3′,4,4′-tetrachlorobiphenyl by a resuscitated strain Castellaniella sp. SPC4: Kinetics model and pathway for biodegradation. Science of the Total Environment, 2019, 688, 917-925.	3.9	40
82	The toxicity of 2,6-dichlorobenzoquinone on the early life stage of zebrafish: A survey on the endpoints at developmental toxicity, oxidative stress, genotoxicity and cytotoxicity. Environmental Pollution, 2019, 245, 719-724.	3.7	40
83	Effects of surface charge on interfacial interactions related to membrane fouling in a submerged membrane bioreactor based on thermodynamic analysis. Journal of Colloid and Interface Science, 2016, 465, 33-41.	5.0	39
84	Bromine incorporation into five DBP classes upon chlorination of water with extremely low SUVA values. Science of the Total Environment, 2017, 590-591, 720-728.	3.9	39
85	Additive-free macroscopic-scale synthesis of coral-like nickel cobalt oxides with hierarchical pores and their electrocatalytic properties for methanol oxidation. Electrochimica Acta, 2014, 145, 300-306.	2.6	38
86	Fractal reconstruction of rough membrane surface related with membrane fouling in a membrane bioreactor. Bioresource Technology, 2016, 216, 817-823.	4.8	37
87	Formation of disinfection by-products during chlorination of organic matter from phoenix tree leaves and Chlorella vulgaris. Environmental Pollution, 2018, 243, 1887-1893.	3.7	37
88	Whole-genome sequencing of an acidophilic Rhodotorula sp. ZM1 and its phenol-degrading capability under acidic conditions. Chemosphere, 2019, 232, 76-86.	4.2	36
89	Effects of ionic strength on membrane fouling in a membrane bioreactor. Bioresource Technology, 2014, 156, 35-41.	4.8	35
90	Regression models evaluating THMs, HAAs and HANs formation upon chloramination of source water collected from Yangtze River Delta Region, China. Ecotoxicology and Environmental Safety, 2018, 160, 249-256.	2.9	35

#	Article	IF	CITATIONS
91	Significantly Enhanced Photocatalytic CO ₂ Reduction by Surface Amorphization of Cocatalysts. Small, 2021, 17, e2102105.	5.2	34
92	Stable and recyclable Fe3C@CN catalyst supported on carbon felt for efficient activation of peroxymonosulfate. Journal of Colloid and Interface Science, 2021, 599, 219-226.	5.0	34
93	Miniaturization of self-assembled solid phase extraction based on graphene oxide/chitosan coupled with liquid chromatography for the determination of sulfonamide residues in egg and honey. Journal of Chromatography A, 2016, 1447, 17-25.	1.8	33
94	Facile large scale fabrication of magnetic carbon nano-onions for efficient removal of bisphenol A. Materials Chemistry and Physics, 2017, 198, 186-192.	2.0	33
95	Plant polyphenols induced the synthesis of rich oxygen vacancies Co3O4/Co@N-doped carbon hollow nanomaterials for electrochemical energy storage and conversion. Journal of Colloid and Interface Science, 2021, 600, 58-71.	5.0	32
96	A novel approach for quantitative evaluation of the physicochemical interactions between rough membrane surface and sludge foulants in a submerged membrane bioreactor. Bioresource Technology, 2014, 171, 247-252.	4.8	31
97	Effects of fractal roughness of membrane surfaces on interfacial interactions associated with membrane fouling in a membrane bioreactor. Bioresource Technology, 2017, 244, 560-568.	4.8	31
98	Highly efficient fluorescent multi-walled carbon nanotubes functionalized with diamines and amides. Journal of Materials Chemistry, 2012, 22, 11912.	6.7	30
99	Using regression models to evaluate the formation of trihalomethanes and haloacetonitriles via chlorination of source water with low SUVA values in the Yangtze River Delta region, China. Environmental Geochemistry and Health, 2016, 38, 1303-1312.	1.8	30
100	Thermodynamic analysis of effects of contact angle on interfacial interactions and its implications for membrane fouling control. Bioresource Technology, 2016, 201, 245-252.	4.8	30
101	Effective decolorization of anthraquinone dye reactive blue 19 using immobilized Bacillus sp. JF4 isolated by resuscitation-promoting factor strategy. Water Science and Technology, 2020, 81, 1159-1169.	1.2	29
102	Adsorption Removal of Various Nitrophenols in Aqueous Solution by Aminopropyl-Modified Mesoporous MCM-48. Journal of Chemical & Engineering Data, 2018, 63, 3606-3614.	1.0	27
103	An iron based organic framework coated with nickel hydroxide for energy storage, conversion and detection. Journal of Colloid and Interface Science, 2021, 600, 150-160.	5.0	27
104	Facile synthesis of halogenated multi-walled carbon nanotubes and their unusual photoluminescence. Journal of Materials Chemistry, 2012, 22, 22113.	6.7	26
105	Ultrathin graphene layer activated dendritic α-Fe2O3 for high performance asymmetric supercapacitors. Journal of Alloys and Compounds, 2019, 780, 212-219.	2.8	26
106	Redox-Triggered Bonding-Induced Emission of Thiol-Functionalized Gold Nanoclusters for Luminescence Turn-On Detection of Molecular Oxygen. ACS Sensors, 2017, 2, 1692-1699.	4.0	25
107	Effect of nitrite on the formation of halonitromethanes during chlorination of organic matter from different origin. Journal of Hydrology, 2015, 531, 802-809.	2.3	24
108	Effects of molecular weight distribution (Md) on the performances of the polyethersulfone (PES) ultrafiltration membranes. Journal of Membrane Science, 2015, 490, 220-226.	4.1	24

#	Article	IF	CITATIONS
109	A novel integrated method for quantification of interfacial interactions between two rough bioparticles. Journal of Colloid and Interface Science, 2018, 516, 295-303.	5.0	24
110	Determination of Sulfonamide Residues in Honey and Milk by HPLC Coupled with Novel Graphene Oxide/Polypyrrole Foam Material-Pipette Tip Solid Phase Extraction. Food Analytical Methods, 2018, 11, 2885-2896.	1.3	24
111	Well dispersed single-walled carbon nanotubes with strong visible fluorescence in water for metal ions sensing. Chemical Communications, 2011, 47, 7167.	2.2	23
112	Binding study of diprophylline with lysozyme by spectroscopic methods. Journal of Luminescence, 2011, 131, 820-824.	1.5	23
113	What is the better choice for Pd cocatalysts for photocatalytic reduction of CO ₂ to renewable fuels: high-crystallinity or amorphous?. Journal of Materials Chemistry A, 2020, 8, 21208-21218.	5.2	23
114	Hollow-structured amorphous prussian blue decorated on graphitic carbon nitride for photo-assisted activation of peroxymonosulfate. Journal of Colloid and Interface Science, 2021, 603, 856-863.	5.0	23
115	The visible photoluminescence mechanism of oxidized multi-walled carbon nanotubes: an experimental and theoretical investigation. Journal of Materials Chemistry C, 2013, 1, 307-314.	2.7	22
116	Experimental evidence for osmotic pressure-induced fouling in a membrane bioreactor. Bioresource Technology, 2014, 158, 119-126.	4.8	22
117	A new strategy to produce low-density polyethylene (LDPE)-based composites simultaneously with high flame retardancy and high mechanical properties. Applied Surface Science, 2018, 437, 75-81.	3.1	22
118	Thermodynamic assessment of adsorptive fouling with the membranes modified via layer-by-layer self-assembly technique. Journal of Colloid and Interface Science, 2017, 494, 194-203.	5.0	21
119	A new approach to construct three-dimensional surface morphology of sludge flocs in a membrane bioreactor. Bioresource Technology, 2016, 219, 521-526.	4.8	20
120	A facile strategy to prepare superhydrophilic polyvinylidene fluoride (PVDF) based membranes and the thermodynamic mechanisms underlying the improved performance. Separation and Purification Technology, 2018, 197, 271-280.	3.9	20
121	Rationally designed Ni ₂ P/Ni/C as a positive electrode for high-performance hybrid supercapacitors. New Journal of Chemistry, 2020, 44, 6810-6817.	1.4	20
122	Quantitative evaluation of the interfacial interactions between a randomly rough sludge floc and membrane surface in a membrane bioreactor based on fractal geometry. Bioresource Technology, 2017, 234, 198-207.	4.8	19
123	Layered Co doped MnO2 with abundant oxygen defects to boost aqueous zinc-ion storage. Journal of Colloid and Interface Science, 2022, 611, 662-669.	5.0	19
124	Quantitative assessment of interfacial interactions with rough membrane surface and its implications for membrane selection and fabrication in a MBR. Bioresource Technology, 2015, 179, 367-372.	4.8	18
125	Integration of Plasmonic Metal and Cocatalyst: An Efficient Strategy for Boosting the Visible and Broadâ€Spectrum Photocatalytic H 2 Evolution. Advanced Materials Interfaces, 2019, 6, 1900775.	1.9	18
126	Amino-Functionalized Mesoporous Silicas MCM-48 as Zn(II) Sorbents in Water Samples. Journal of Chemical & Engineering Data, 2012, 57, 2059-2066.	1.0	17

#	Article	IF	CITATIONS
127	Regulating the electronic structure of Fe-based metal organic frameworks by electrodeposition of Au nanoparticles for electrochemical overall water splitting. Journal of Colloid and Interface Science, 2022, 626, 426-434.	5.0	17
128	Dual active sites of the Co ₂ N and single-atom Co–N ₄ embedded in nitrogen-rich nanocarbons: a robust electrocatalyst for oxygen reduction reactions. Nanotechnology, 2020, 31, 165401.	1.3	16
129	Effective biological nitrogen process and nitrous oxide emission characteristics for the treatment of landfill leachate with low carbon-to-nitrogen ratio. Journal of Cleaner Production, 2020, 268, 122289.	4.6	16
130	TEA driven C, N co-doped superfine Fe3O4 nanoparticles for efficient trifunctional electrode materials. Journal of Colloid and Interface Science, 2022, 609, 249-259.	5.0	16
131	Ultrasound-assisted dispersive liquid–liquid microextraction based on solidification of floating organic droplets coupled with gas chromatography for the determination of pesticide residues in water samples. Analytical Methods, 2014, 6, 3388.	1.3	15
132	Synthesis and Functionalization of Stable and Bright Copper Nanoclusters by In Situ Generation of Silica Shells for Bioimaging and Biosensing. ACS Applied Nano Materials, 2018, 1, 5673-5681.	2.4	15
133	Chronic exposure to dichloroacetamide induces biochemical and histopathological changes in the gills of zebrafish. Environmental Toxicology, 2019, 34, 781-787.	2.1	15
134	Modeling and predicting pKa values of mono-hydroxylated polychlorinated biphenyls (HO-PCBs) and polybrominated diphenyl ethers (HO-PBDEs) by local molecular descriptors. Chemosphere, 2015, 138, 829-836.	4.2	14
135	Magnetic Metal-Organic Framework/Graphene Oxide-Based Solid-Phase Extraction Combined with Spectrofluorimetry for the Determination of Enrofloxacin in Milk Sample. Food Analytical Methods, 2017, 10, 4094-4103.	1.3	13
136	Simple and sensitive detection method for diprophylline using glutathione-capped CdTe quantum dots as fluorescence probes. Journal of Luminescence, 2014, 145, 575-581.	1.5	12
137	Multicolour fluorescent graphene oxide by cutting carbon nanotubes upon oxidation. CrystEngComm, 2012, 14, 4976.	1.3	11
138	Membrane fouling in a submerged membrane bioreactor: An unified approach to construct topography and to evaluate interaction energy between two randomly rough surfaces. Bioresource Technology, 2017, 243, 1121-1132.	4.8	11
139	Metallic cobalt and molybdenum oxides encapsulated in B, N-doped carbon nanocomposite catalyzed hydrogen evolution from ammonia borane hydrolysis. Vacuum, 2020, 174, 109213.	1.6	11
140	Ultra-Preconcentration and Determination of Multiple Pesticide Residues in Water Samples Using Ultrasound-Assisted Dispersive Liquid–Liquid Microextraction and GC-FID. Chromatographia, 2013, 76, 671-678.	0.7	10
141	Viscosity-sensitive thiolated gold nanoclusters with diffusion-controlled emission for intracellular viscosity imaging. Analyst, The, 2019, 144, 4483-4487.	1.7	10
142	Adsorption of Methyl Violet Onto Mesoporous MCM-48 from Aqueous Solution. Journal of Nanoscience and Nanotechnology, 2014, 14, 4655-4663.	0.9	9
143	Coordinate bonding-induced emission of gold-glutathione complex for sensitive detection of aluminum species. Sensors and Actuators B: Chemical, 2018, 272, 1-7.	4.0	9
144	Tuning the energy barrier of water exchange reactions on Al(iii) by interaction with the single-walled carbon nanotubes. Dalton Transactions, 2011, 40, 4183.	1.6	6

#	Article	IF	CITATIONS
145	Theoretical investigation of the dissociative interchange (Id) mechanism for water exchange on magnesium(II) in aqueous solution. Inorganica Chimica Acta, 2010, 363, 3627-3631.	1.2	5
146	Thermodynamic insights into membrane fouling in a membrane bioreactor: Evaluating thermodynamic interactions with Gaussian membrane surface. Journal of Colloid and Interface Science, 2018, 527, 280-288.	5.0	5
147	Adsorption of multi-bivalent heavy metal ions in aqueous solution onto aminopropyl-functionalized MCM-48 preparation by co-condensation. Separation Science and Technology, 2021, 56, 1819-1829.	1.3	5
148	Unusual visible luminescence of aluminium polyoxocations in aqueous solution. Chemical Communications, 2011, 47, 12652.	2.2	4
149	Author's responses to the comment by Seong-Hoon Yoon on "A new insight into membrane fouling mechanism in submerged membrane bioreactor: Osmotic pressure during cake layer filtration― published in Water Research, vol. 47, pp.Â2777–2786, 2013. Water Research, 2013, 47, 4790-4791.	5.3	3
150	One-Pot and Surfactant-Free Synthesis of Ultrafine PtSn Nanoparticles Supported on Onion-Like Nanocarbons Toward Efficient Methanol and Ethylene Glycol Oxidation Reactions. Journal of Nanoscience and Nanotechnology, 2020, 20, 2408-2415.	0.9	3